Journal of Engineering Mathematics 19 (1985) 329–339.

A numerical method for non-linear flow about a submerged hydrofoil

L.K. FORBES *

Department of Mathematics, Kansas State University, Manhattan, KS 66506, USA

(Received June 4, 1985)

Summary

A numerical method is presented for computing two-dimensional potential flow about a wing with a cusped trailing edge immersed beneath the free surface of a running stream of infinite depth. The full non-linear boundary conditions are retained at the free surface of the fluid, and the conditions on the hydrofoil are also stated exactly. The problem is solved numerically using integral-equation techniques combined with Newton's method. Surface profiles and the pressure distribution on the body are shown for different body geometries.

1. Introduction

This paper is concerned with the flow of an ideal fluid about a hydrofoil immersed beneath the free surface. The fluid is of infinite depth and flows steadily from left to right. The hydrofoil is assumed to possess a blunt nose and a cusped trailing edge.

Linearized theories may be developed by regarding the hydrofoil thickness as a small parameter. This approach is summarized by Wehausen and Laitone ([1], page 583). As in the case of thin-wing aerofoil theory, an integral equation is obtained for the strengths of the vortices distributed along the centre-line of the foil; however, unlike classical aerofoil theory, there is no simple closed-form solution to this equation. Nevertheless, it is still possible to demonstrate that the application of the Kutta condition at the trailing edge gives a bounded fluid velocity there, but an infinite velocity at the leading edge.

A numerical investigation of the non-linear potential flow about a hydrofoil has been undertaken by Salvesen and von Kerczek [2]. They solved Laplace's equation in a fluid of fixed finite depth using finite differences; clearly, such an approach is not directly available in the conceptually simpler case of infinite depth considered here. In addition, finite-difference methods are obviously difficult to apply in irregularly-shaped computational domains. However, the authors are able to claim reasonable agreement with experimental data. Further numerical techniques for linearized and non-linear free-surface problems are reviewed by Yeung [3], and the review article by Acosta [4] surveys the general field of hydrofoil vehicles.

* Presently on leave at: Department of Mathematics, University of Queensland, St. Lucia 4067, Queensland, Australia.

In this paper, the physical-plane integral-equation approach of Forbes [5] is used to formulate the fully non-linear potential-flow problem in infinitely deep fluid. The numerical approximation of the flow equations then only involves mesh points distributed on the hydrofoil and on a portion of the free surface. These equations are solved by an efficient numerical method in which Newton's method is used to find only the unknowns at the free surface, and the unknowns on the hydrofoil surface are updated at each iteration of Newton's method.

Our aims in the present paper are two-fold; firstly, we wish to present the current numerical scheme as a competitive method for the solution of problems of this type. The second aim concerns the fact that recent numerical work by von Kerczek and Salvesen [6], Schwartz [7] and Forbes [5,8,9] has shown that non-linear, *drag-free* solutions to water-wave problems are possible under certain circumstances, and we wish to establish whether or not such solutions are possible in the present problem also.

2. Formulation of the problem

We consider a fluid of infinite depth flowing with speed c from left to right, under the influence of the downward acceleration g of gravity. A cartesian coordinate system is located with the x-axis lying along the undisturbed surface and pointing in the direction of flow, and the y-axis pointing vertically. Now let an aerofoil of length $2L$ and width $2B$ be placed a distance H beneath the origin of the previously-defined coordinate system; the upper and lower surfaces of the foil are given by the equations $y = b_{\pm}(x)$, $-L \leqslant x \leqslant L$, and the disturbed free surface now has the location $y = \eta(x)$.

The speed c and depth H are used as reference quantities with which to render the problem dimensionless. With this choice of non-dimensional coordinates, the solutions are seen to be dependent upon the three dimensionless parameters $F = c(gH)^{-1/2}$ the Froude number based on submergence depth, $\alpha = L/H$ the foil half-length, and $\beta = B/H$ its half-width. Since the fluid is ideal and flows irrotationally, its horizontal and vertical components of velocity u and v are able to be described in terms of a velocity potential ϕ and streamfunction ψ according to the Cauchy-Riemann equations

$$u = \phi_x = \psi_y, \quad v = \phi_y = -\psi_x. \tag{2.1}$$

Far upstream, the fluid velocity satisfies the radiation condition

$$u \to 1, \; v \to 0 \qquad \text{as} \quad x \to -\infty, \tag{2.2}$$

and on the body, the requirement that there be no normal component of velocity gives

$$v_{\pm} = u_{\pm} b'_{\pm}(x) \qquad \text{on} \quad y = b_{\pm}(x), \quad -\alpha \leqslant x \leqslant \alpha, \tag{2.3}$$

where the $+$ and $-$ subscripts denote the upper and lower surfaces of the hydrofoil, respectively. On the free surface of the fluid, the usual kinematic and Bernoulli equations are imposed; specifically,

$$u\eta'(x) = v, \quad \tfrac{1}{2}F^2(u^2 + v^2) + y = \tfrac{1}{2}F^2 \qquad \text{on} \quad y = \eta(x). \tag{2.4}$$

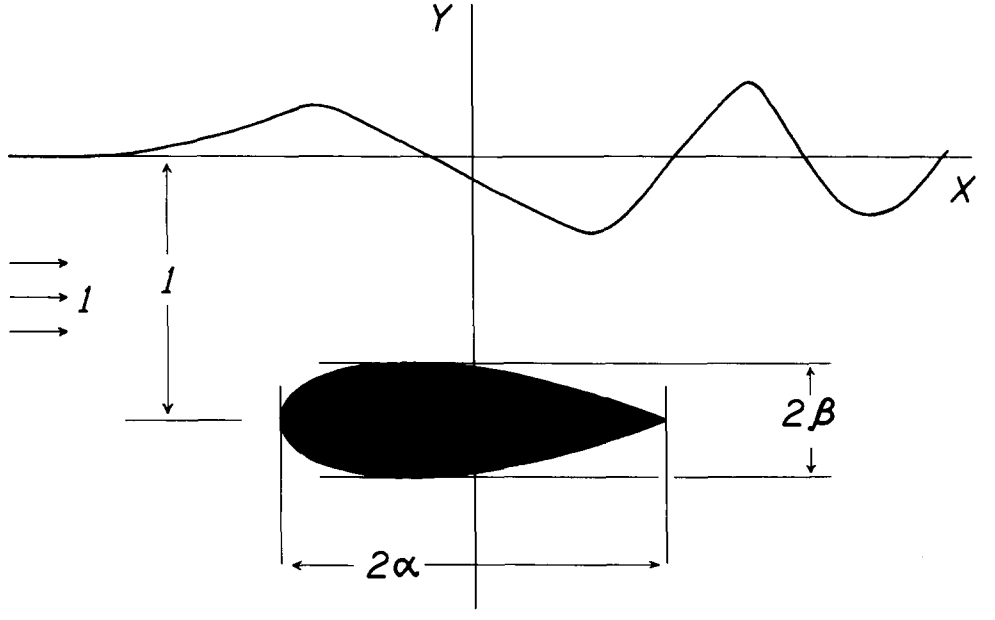

Figure 1. The dimensionless flow configuration, showing the assumed shape of the hydrofoil.

It remains to choose a specific shape for the body. We shall consider the symmetric foil with zero attack angle described by the functions

$$b_{\pm}(x) = -1 \pm \tfrac{3}{4}\beta\left(1 - \frac{x}{\alpha}\right)\sqrt{\tfrac{3}{2}\left(1 + \frac{x}{\alpha}\right)}, \quad -\alpha \leqslant x \leqslant \alpha. \tag{2.5}$$

This is a body with a blunt nose and a cusped trailing edge, and which achieves its maximum width 2β when $x = -\alpha/3$. The hydrofoil shape and a schematic illustration of the flow are given in Fig. 1. At the trailing edge, we must impose the Kutta condition

$$u_+ = u_-, \; v_+ = v_- = 0 \qquad \text{at} \quad x = \alpha, \tag{2.6}$$

which is a statement that the flow leaves the foil tangentially.

An integral-equation approach is now used to reformulate the problem. The derivation is similar to that given in Forbes [5] except that now there are two integral equations involved at the free surface and at the body. Accordingly, we shall omit some of the details.

We observe that, in view of equations (2.1), the complex potential $f = \phi + \mathrm{i}\psi$ is an analytic function of $z = x + \mathrm{i}y$, and so Cauchy's Integral Formula is applied to the analytic function

$$\chi(z) = \frac{\mathrm{d}f}{\mathrm{d}z} - 1$$

in the doubly-connected fluid domain, on a contour consisting of the entire free surface, the body, and a semi-circle infinitely deep within the fluid, centred at the origin. The free surface is parametrized using arclength s, in terms of which the kinematic and Bernoulli equations (2.4) become

$$\psi_s = 0 \tag{2.7}$$

and

$$\tfrac{1}{2}F^2\phi_s^2 + y = \tfrac{1}{2}F^2. \tag{2.8}$$

In addition, the definition of arclength s requires that

$$x_s^2 + y_s^2 = 1. \tag{2.9}$$

Suppose that a fixed point on the free surface has the value of arclength s, and that a moving point has arclength t. In order to apply Cauchy's Integral formula, the point $z(s)$ on the free surface must be by-passed with a semi-circle of vanishingly small radius, from which the contribution to the integral is $-\pi i\chi(z(s))$; consequently, we obtain

$$\pi i\chi(z(s)) = -\int_{-\infty}^{\infty} \frac{\chi(z(t))z'(t)\mathrm{d}t}{z(t)-z(s)} + \oint_{\text{body}} \frac{\chi(\lambda)\mathrm{d}\lambda}{\lambda - z(s)}, \tag{2.10}$$

where the integral around the body is to be taken in the negative (clockwise) sense. The contribution from the semi-circle at infinity is zero, since $\chi(z) = 0$ there, and the improper integral in equation (2.10) is to be interpreted as Cauchy principal valued for $t \to s$.

The complex number $\lambda = x + ib_{\pm}(x)$ in equation (2.10) defines a location on the hydrofoil, and so the body-integral may be re-written as

$$\int_{-\alpha}^{\alpha} \frac{(u_+ - 1 - iv_+)(1 + ib'_+)\mathrm{d}\xi}{\xi + ib_+ - z(s)} - \int_{-\alpha}^{\alpha} \frac{(u_- - 1 - iv_-)(1 + ib'_-)\mathrm{d}\xi}{\xi + ib_- - z(s)}.$$

In order to cope with the inverse square-root singularities in these integrands as $x \to -\alpha$, introduced by the functions $b'_{\pm}(x)$, we make the change of variable

$$x = k^2 - \alpha \tag{2.11}$$

on the body surface. In addition, we define

$$\begin{aligned} b_{\pm}(x) &\equiv B_{\pm}(k) = -1 \pm \tfrac{3}{4}\beta\sqrt{\frac{3}{2\alpha}}\, k\left(2 - \frac{k^2}{\alpha}\right), \\ b'_{\pm}(x) &\equiv D_{\pm}(k) = \pm\frac{3\beta}{8\alpha}\sqrt{\frac{3}{2\alpha}}\left(\frac{2\alpha - 3k^2}{k}\right). \end{aligned} \tag{2.12}$$

The desired integrodifferential equation for a point on the free surface is obtained by

taking the real part of equation (2.10), and making use of (2.3), (2.7) and (2.9). This gives

$$\pi[\phi'(s)x'(s)-1]$$
$$=\int_{-\infty}^{\infty}\frac{[\phi'(t)-x'(t)][y(t)-y(s)]+y'(t)[x(t)-x(s)]}{[x(t)-x(s)]^2+[y(t)-y(s)]^2}\,dt$$
$$-2\int_0^{\sqrt{2\alpha}}\frac{[B_+(K)-y(s)][u_+-1+v_+D_+]+[K^2-\alpha-x(s)]D_+(K)}{[K^2-\alpha-x(s)]^2+[B_+(K)-y(s)]^2}K\,dK$$
$$+2\int_0^{\sqrt{2\alpha}}\frac{[B_-(K)-y(s)][u_--1+v_-D_-]+[K^2-\alpha-x(s)]D_-(K)}{[K^2-\alpha-x(s)]^2+[B_-(K)-y(s)]^2}K\,dK. \tag{2.13}$$

The derivation of the integrodifferential equation for points on the hydrofoil follows the same steps as outlined above. The resulting equation is

$$\pi C[u_\pm(k)-1]$$
$$=\int_{-\infty}^{\infty}\frac{[\phi'(t)-x'(t)][y(t)-B_\pm(k)]+y'(t)[x(t)-k^2+\alpha]}{[x(t)-k^2+\alpha]^2+[y(t)-B_\pm(k)]^2}\,dt$$
$$-2\int_0^{\sqrt{2\alpha}}\frac{[B_+(K)-B_\pm(k)][u_+-1+v_+D_+]+(K^2-k^2)D_+(K)}{(K^2-k^2)^2+[B_+(K)-B_\pm(k)]^2}K\,dK$$
$$+2\int_0^{\sqrt{2\alpha}}\frac{[B_-(K)-B_\pm(k)][u_--1+v_-D_-]+(K^2-k^2)D_-(K)}{(K^2-k^2)^2+[B_-(K)-B_\pm(k)]^2}K\,dK. \tag{2.14}$$

The constant C has the value 1, except when $k=\sqrt{2\alpha}$, which is the position of the cusped trailing edge, which we shall assume encloses an angle γ. In this special case, C has the value $2-\gamma/\pi$. Note that equation (2.14) applies on both the upper and lower surfaces of the foil.

The solution to this problem consists of finding the functions $x(s)$, $y(s)$ and $\phi(s)$ at the free surface, and $u_\pm(k)$ and $v_\pm(k)$ at the body. The governing equations are (2.3), (2.8), (2.9), (2.13) and (2.14), subject to the radiation condition (2.2) and the Kutta condition (2.6).

The drag and lift may now be computed from the solution to the above problem, using the Blasius formula. In the case of the drag R, this yields

$$R=F^2\int_0^{\sqrt{2\alpha}}\left[\left(u_-^2+v_-^2\right)D_--\left(u_+^2+v_+^2\right)D_+\right]k\,dk. \tag{2.15}$$

An alternative method for the determination of wave resistance R comes from straightfor-

ward momentum conservation in any control volume containing the hydrofoil. If $x = x_w$ denotes a vertical line in the downstream wave field, then

$$R = \tfrac{1}{2}\eta^2(x_w) + \tfrac{1}{2}F^2\int_{-\infty}^{\eta(x_w)}\left[v^2 - (u-1)^2\right](x_w, y)\,dy. \tag{2.16}$$

Since equation (2.16) is less sensitive than (2.15) to velocity gradients on the hydrofoil surface, it usually yields more accurate results, although it does require the determination of u and v at a line of points downstream, using the Cauchy Integral Formula. Once these have been determined, however, they provide the additional advantage of supplying a check on the accuracy of the computed solution, using the conservation of mass result

$$\int_{-\infty}^{\eta(x_w)}\left[u(x_w, y) - 1\right]dy + \eta(x_w) = 0. \tag{2.17}$$

3. Numerical methods

The method used here to obtain numerical values of the unknowns at the surface and at the body is a modification of that given by Forbes [5]. Points are chosen at the N equally-spaced values of the surface arclength $s_1, s_2, \ldots, s_N$, with point spacing $\Delta s = (s_N - s_1)/(N-1)$. Similarly, M body points $k_1, k_2, \ldots, k_M$ are chosen, with uniform spacing $\Delta k = (k_M - k_1)/(M-1)$ in the variable k defined in equation (2.11). The unknown functions $x(s)$, $y(s)$ and $\phi(s)$ at the free surface are represented by point values x_i, y_i and ϕ_i, $i = 1, \ldots, N$, and on the body, the functions $u_+(k)$, $u_-(k)$, $v_+(k)$ and $v_-(k)$ are represented as u_i^+, u_i^-, v_i^+ and v_i^-, $i = 1, \ldots, M$.

The radiation condition (2.2) is imposed at the first surface point, in a manner which also satisfies Bernoulli's equation there, by specifying

$$y_1 = y_1' = 0, \quad x_1' = \phi_1' = 1, \quad x_1 = \phi_1 = s_1. \tag{3.1}$$

The body condition (2.3) is imposed at the nose, and the Kutta condition (2.6) specified at the trailing edge, to give

$$\begin{aligned} &u_1^+ = u_1^- = 0, \quad v_1^+ = v_1^- \equiv v_1^{\pm}; \\ &u_M^+ = u_M^- \equiv u_M^{\pm}, \quad v_M^+ = v_M^- = 0. \end{aligned} \tag{3.2}$$

The integral equations (2.13) and (2.14) are evaluated at the half-mesh points $s_{i-1/2}$, $i = 2, \ldots, N$, and $k_{i-1/2}$, $i = 2, \ldots, M$, and the integrals are approximated by the trapezoidal rule, ignoring the symmetrically-placed singularity as described by Monacella [10]. This yields a system of $N + 2M - 3$ non-linear, algebraic equations.

Newton's method is used to solve this system, by proceeding in the following manner. To begin, values of the dependent variables at the halfpoints $s_{i-1/2}$ and $k_{i-1/2}$ are interpolated onto whole-mesh values according to formulae of the type

$$x_{i-1/2} = \tfrac{1}{2}(x_{i-1} + x_i), \quad i = 2, \ldots, N,$$

etc. on the surface, and

$$u^+_{i-1/2} = \tfrac{1}{2}(u^+_{i-1} + u^+_i), \quad i = 2, \ldots, M,$$

etc. on the body. An initial guess is now made for the vector $[y'_2 y'_3 \ldots y'_N]^T$ of surface unknowns; these are usually set to zero. These approximate values of y'_i, $i = 2, \ldots, N$, are sufficient to determine all the other dependent functions at the free surface, using equations (2.8), (2.9) and trapezoidal-rule integration. Thus

$$\begin{aligned}
x'_i &= \left(1 - y'^2_i\right)^{1/2}, \\
x_i &= x_{i-1} + \tfrac{1}{2}\Delta s(x'_i + x'_{i-1}), \\
y_i &= y_{i-1} + \tfrac{1}{2}\Delta s(y'_i + y'_{i-1}), \\
\phi'_i &= \left(1 - \frac{2y_i}{F^2}\right)^{1/2}, \\
\phi_i &= \phi_{i-1} + \tfrac{1}{2}\Delta s(\phi'_i + \phi'_{i-1}), \quad i = 2, \ldots, N.
\end{aligned} \tag{3.3}$$

Now that approximate values for all the surface variables are known from equations (3.3), the $2M - 2$ algebraic equations which approximate the body integral equation (2.14) can be inverted immediately to yield the values of the dependent variables at the hydrofoil. In view of the conditions (3.2), we define the vector $\boldsymbol{U} = [v_1^{\pm} u_2^+ \ldots u_{M-1}^+ u_M^{\pm} u_2^- \ldots u_{M-1}^-]^T$ of body values, eliminating the vertical components of velocity using equations (2.3) written in the form

$$v_i^+ = u_i^+ D_+(k_i), \quad v_i^- = u_i^- D_-(k_i), \quad i = 2, \ldots, M-1. \tag{3.4}$$

Equation (2.14) yields the matrix system

$$\boldsymbol{SU} = \boldsymbol{TU} + \boldsymbol{R}, \tag{3.5}$$

where $\boldsymbol{S}$ and $\boldsymbol{T}$ are $(2M-2)\times(2M-2)$ matrices and $\boldsymbol{R}$ is a vector of length $2M-2$ which depends on variables at the free surface. Since $(\boldsymbol{S} - \boldsymbol{T})^{-1}$ is a matrix which is independent of the changing surface values, it is stored at the beginning of the program and not recomputed.

Equations (3.1)–(3.5) provide values for all the unknown functions, once an estimate has been made for the vector $[y'_2 \ldots y'_N]^T$. This estimate is improved using Newton's method. The integral equation (2.13) at the surface provides a system of $N - 1$ algebraic equations of the form

$$E_i(y'_2, y'_3, \ldots, y'_N) = 0, \quad i = 2, \ldots, N, \tag{3.6}$$

from which a correction vector $[\Delta_2 \Delta_3 \ldots \Delta_N]^T$ is computed by solving the matrix equation

$$\sum_{j=2}^{N} \frac{\partial E_i}{\partial y'_j} \Delta_j = -E_i, \quad i = 2, \ldots, N. \tag{3.7}$$

The Jacobian matrix of derivatives in equation (3.7) is evaluated by forward differencing of (3.6), and the vector $[y_2' \dots y_N']^T$ is updated by adding to it the correction vector $[\Delta_2 \dots \Delta_N]^T$.

This algorithm has been programmed on an NAS 6630 computer, and generally converges to a highly accurate solution of the algebraic equations within five iterations of Newton's method. When $N = 121$ and $M = 101$, a total of 321 points, the programme takes about 40 minutes execution time.

4. Presentation of results

Figure 2 shows typical free-surface profiles computed with the present method. Here, $F = 0.7$ and $\alpha = 1$, and the two profiles correspond to the two values of foil half-width $\beta = 0.05$ and $\beta = 0.15$. There are slight errors in the wave profiles due to the truncation of the free surface upstream at s_1 and downstream at s_N; these errors are manifested as a small wave train ahead of the foil and an inaccuracy in the last half wavelength downstream. Detailed descriptions of these numerical errors are given by Forbes and Schwartz [11] and Forbes [5], and the subject will not be discussed further here. Notice, however, that the familiar features of non-linear two-dimensional surface waves are present here; the wave crests are (slightly) more peaked than the troughs, and there is a shortening of wavelength with increasing wave height. The first wave downstream is noticeably higher than the rest, and there is in addition a substantial rise in the free surface at the approximate position of the nose of the hydrofoil.

The pressure P on the hydrofoil is also of interest, and can be computed from our numerical solutions using Bernoulli's equation

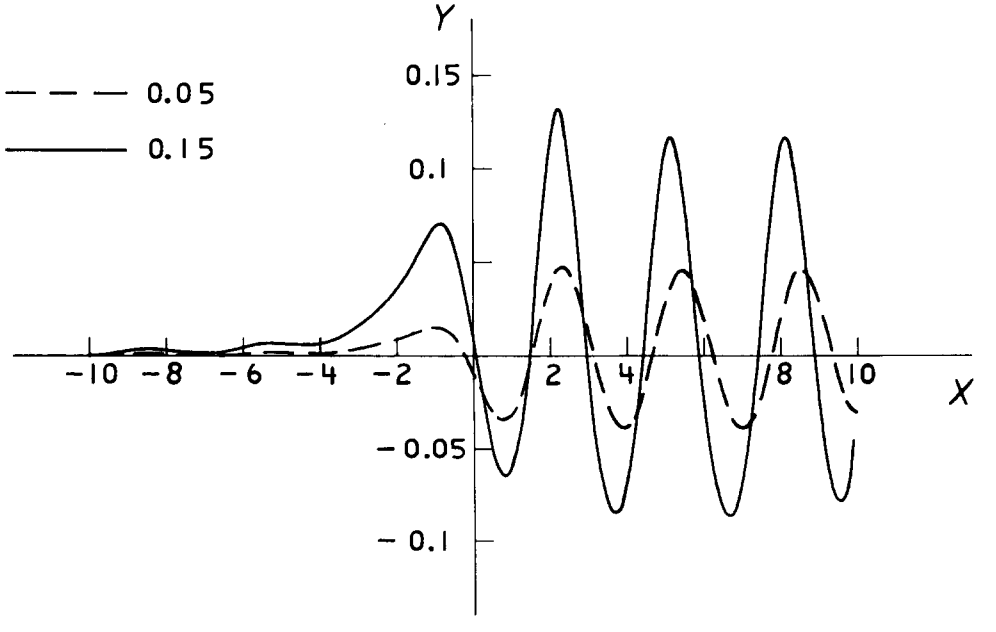

Figure 2. Free-surface profiles for $F = 0.7$, $\alpha = 1$ and the two different values of foil half-width $\beta = 0.05$ and $\beta = 0.15$.

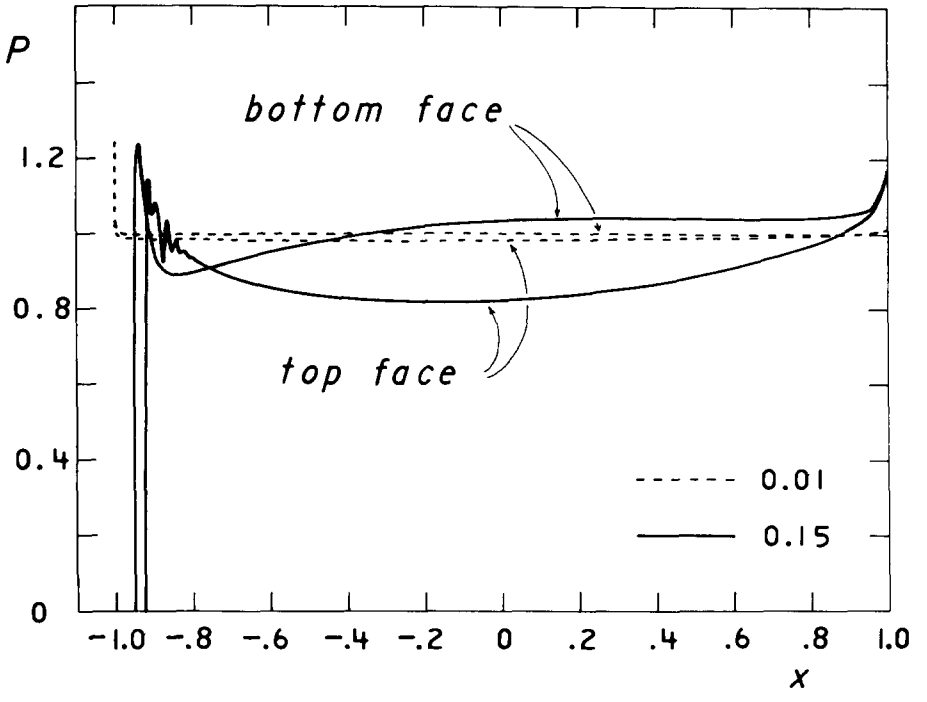

Figure 3. Pressure on the hydrofoil as a function of x, for $F = 0.7$, $\alpha = 1$. Results are shown for $\beta = 0.01$ and $\beta = 0.15$.

$$P = \tfrac{1}{2}F^2 - y - \tfrac{1}{2}F^2(u^2 + v^2).$$

This quantity is shown in Fig. 3 as a function of x, for $F = 0.7$ and $\alpha = 1$, and the two foil half-widths $\beta = 0.01$ and $\beta = 0.15$. When $\beta = 0.01$, the foil is extremely thin, having degenerated almost to the branch cut assumed by linearized theory. Nevertheless, an important difference exists between the qualitative predictions of linearized theory and the results for $\beta = 0.01$ presented in Fig. 3. It will be recalled that linearized theory predicts infinite fluid velocity at the leading edge, and consequently, negative infinite pressure there. It is usually assumed that this is due to the fact that such theories ignore the presence of the stagnation point at the leading edge; this assumption would appear to be confirmed by the results for $\beta = 0.01$ in Fig. 3, in which the pressure rises abruptly to the stagnation value 1.245 at the nose $x = -1$.

The pressure profile in Fig. 3 for the half-width $\beta = 0.15$ indicates a rather different flow pattern at the nose than for the case $\beta = 0.01$. Observe that the stagnation pressure is attained on the lower face of the hydrofoil at about $x = -9.4$, indicating a fluid stagnation point at this location, rather than at the nose. Indeed the vertical component of velocity at the nose is very large and the pressure consequently has large negative values there. On the top face of the hydrofoil, the pressure profile exhibits a small region of sawtooth behaviour near the nose. This is evidence of numerical inaccuracy in this very unstable region of the flow, and could be reduced by utilizing more grid points on the hydrofoil. However, we have employed 101 points on each face of the foil, and are already using our computing facilities to their practical limit.

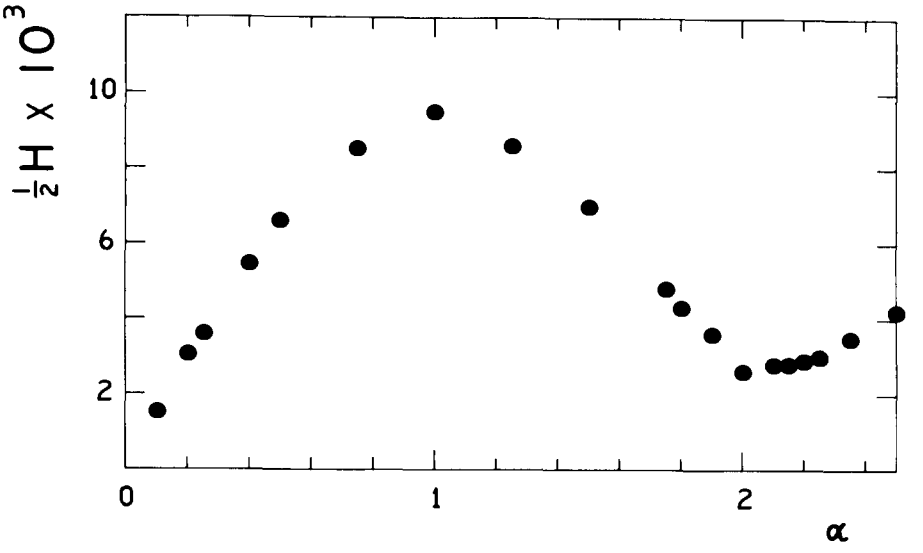

Figure 4. Downstream wave "amplitude" as a function of foil half-length α, when $F = 0.7$ and $\beta = 0.01$.

As stated in the introduction, a major aim of the present study is to determine whether non-linear, *drag-free* solutions of the type described by Forbes [8,9] are possible in this problem. To do this, we have run our computer programme for nineteen different values of the foil half-length α, in the case when $F = 0.7$, $\beta = 0.01$, and the results are shown in Fig. 4. Here, in order to reduce computing time, we have taken $N = 121$ free-surface points, but only $M = 51$ foil points, giving a total of 221 grid points overall. This reduced accuracy at the hydrofoil has little effect on the free-surface profiles, but results in a sawtooth numerical error in values of u and v on the foil, similar to that seen in Fig. 3. Consequently equation (2.15) cannot be used for the determination of the wave resistance R, and even (2.16) yields results of doubtful accuracy. We have therefore defined the quantity H to be the peak-trough wave height estimated from our free-surface profiles, and show the "amplitude" $\frac{1}{2}H$ as a function of foil half-length α in Fig. 4. It is clear that the downstream wave height H exhibits the familiar maxima and minima of many such wave-resistance plots; in addition, the work of Forbes [8,9] suggests that the values of α at which these extrema occur are likely to be strong functions of the foil half-width β. Nevertheless, the local minimum which occurs at about $\alpha = 2.1$ differs from zero, and we conclude that zero drag solutions are probably impossible for this problem.

5. Concluding remarks

Numerical solutions have been obtained for fully non-linear, two-dimensional, potential flow about a hydrofoil submerged beneath a free surface. We have used an extremely efficient numerical method in which only the free-surface location is sought explicitly, and the velocity components on the body are then updated at each iteration.

The numerical results suggest that non-linear, *drag-free* solutions do not exist for this problem. Of course, we have only investigated the case of a hydrofoil at zero angle of attack, and it may be possible to find them at other attack angles. Definite minima in the

wave resistance do occur at certain values of the foil half-length α, and the accurate determination of these values is expected to be of practical use in the design of hydrofoil craft.

References

[1] J.V. Wehausen and E.V. Laitone, Surface waves, in: *Handbuch der Physik*, vol. 9, Springer-Verlag (1960).

[2] N. Salvesen and C.H. von Kerczek, Numerical solutions of two-dimensional nonlinear body-wave problems, *Proc. 1st. Int. Conf. on Numerical Ship Hydrodynamics* (1975) 279–293.

[3] R.W. Yeung, Numerical methods in free-surface flows, *Ann. Rev. Fluid Mech.* 14 (1982) 395–442.

[4] A.J. Acosta, Hydrofoils and hydrofoil craft, *Ann. Rev. Fluid Mech.* 5 (1973) 161–184.

[5] L.K. Forbes, On the effects of non-linearity in free-surface flow about a submerged point vortex, *J. Engineering Maths.* 19 (1985) 139–156.

[6] C. von Kerczek and N. Salvesen, Nonlinear free-surface effects - the dependence on Froude number, *Proc. 2nd. Int. Conf. on Numerical Ship Hydrodynamics* (1977) 292–300.

[7] L.W. Schwartz, Nonlinear solution for an applied overpressure on a moving stream, *J. Engineering Maths.* 15 (1981) 147–156.

[8] L.K. Forbes, On the wave resistance of a submerged semi-elliptical body, *J. Engineering Maths.* 15 (1981) 287–298.

[9] L.K. Forbes, Non-linear, drag-free flow over a submerged semi-elliptical body, *J. Engineering Maths.* 16 (1982) 171–180.

[10] V.J. Monacella, On ignoring the singularity in the numerical evaluation of Cauchy Principal Value integrals, *Hydromechanics laboratory research and development report no. 2356, David Taylor Model Basin, Washington, DC.* (1967).

[11] L.K. Forbes and L.W. Schwartz, Free-surface flow over a semicircular obstruction, *J. Fluid Mech.* 114 (1982) 299–314.